Research in Pharmaceutical Sciences, August 2023; 18(4): 358-370
Received: 30-08-2022
Peer Reviewed: 12-11-2022
Revised: 20-11-2022
Accepted: 23-05-2023
Published: 01-06-2023

School of Pharmacy & Pharmaceutical Sciences
Isfahan University of Medical Sciences

Original Article

Chemoprevention curcumin analog 1.1 promotes metaphase arrest and enhances intracellular reactive oxygen species levels on TNBC MDA-MB-231 and HER2-positive HCC1954 cells

Dhania Novitasari[1], Riris Istighfari Jenie[1,2], Jun-ya Kato[3], and Edy Meiyanto[1,2,*]

[1]Cancer Chemoprevention Research Center, Faculty of Pharmacy, Universitas Gadjah Mada, Yogyakarta, Indonesia.
[2]Department of Pharmaceutical Chemistry, Faculty of Pharmacy, Universitas Gadjah Mada, Yogyakarta, Indonesia.
[3]Division of Biological Science, Graduate School of Science and Technology, Nara Institute of Science and Technology, Nara, Japan.

Abstract

Background and purpose: Previous studies highlighted that chemoprevention curcumin analog-1.1 (CCA-1.1) demonstrated an antitumor effect on breast, leukemia, and colorectal cancer cells. By utilizing immortalized MDA-MB-231 and HCC1954 cells, we evaluated the anticancer properties of CCA-1.1 and its mediated activity to promote cellular death.

Experimental approach: Cytotoxicity and anti-proliferation were assayed using trypan blue exclusion. The cell cycle profile after CCA-1.1 treatment was established through flow cytometry. May-Grünwald-Giemsa and Hoechst staining were performed to determine the cell cycle arrest upon CCA-1.1 treatment. The involvement of CCA-1.1 in mitotic kinases (aurora A, p-aurora A, p-PLK1, and p-cyclin B1) expression was investigated by immunoblotting. CCA-1.1-treated cells were stained with the X-gal solution to examine the effect on senescence. ROS level and mitochondrial respiration were assessed by DCFDA assay and mitochondrial oxygen consumption rate, respectively.

Findings/Results: CCA-1.1 exerted cytotoxic activity and inhibited cell proliferation with an irreversible effect, and the flow cytometry analysis demonstrated that CCA-1.1 significantly halted during the G2/M phase, and further assessment revealed that CCA-1.1 caused metaphase arrest. Immunoblot assays confirmed CCA-1.1 suppressed aurora A kinase in MDA-MB-231 cells. The ROS level was elevated after treatment with CCA-1.1, which might promote cellular senescence and suppress basal mitochondrial respiration in MDA-MB-231 cells.

Conclusion and implications: Our data suggested the *in vitro* proof-of-concept that supports the involvement in cell cycle regulation and ROS generation as contributors to the effectiveness of CCA-1.1 in suppressing breast cancer cell growth.

Keywords: Breast cancer cells; Curcumin derivative; Metaphase arrest; ROS generation.

INTRODUCTION

Chemoprevention curcumin analog 1.1 (CCA-1.1; Fig. 1), a novel curcumin derivative synthesized based on a reduction reaction from pentagamavunone-1 (PGV-1) (1), has been reported for its cytotoxic activity against luminal breast, colorectal, and leukemia cancer cells. Known mediated cellular mechanisms had been revealed upon CCA-1.1 in cancer cells, such as inducing G2/M cell arrest and cellular senescence and enhancing reactive oxygen species (ROS) generation (2-4). Moreover, a recent study determined the possible targets of CCA-1.1 in mitotic regulators (aurora A, CDK1, PLK1, KIF11) using bioinformatic analysis (5-7) later demonstrated that CCA-1.1 had a cytotoxic and synergistic effect with PGV-1 to eliminate K562 cells. For these reasons, the exploration of elucidating the molecular mechanism of CCA-1.1 in cell cycle arrest becomes essential.

*Corresponding author: E. Meiyanto
Tel: +62-274543120, Fax: +62-274543120
Email: edy_meiyanto@ugm.ac.id

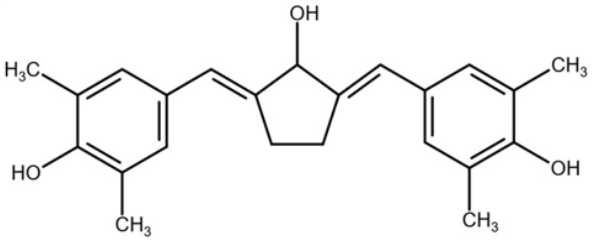

Fig. 1. Chemical structure of CCA-1.1.

Recent studies have already documented the specific phenomenon when chemotherapy drugs delay cancer cells during G2, then prematurely enter mitosis to induce later mitotic catastrophe (8,9). Mitotic catastrophe is believed to be the initial stage before mitotic arrest, and prolonged arrest can either proceed to senescence or apoptosis (10). Moreover, the high heterogeneity of breast tumors also impacted the genome instability and aneuploidy of cells due to the loss or gain of function of p53. Mitotic catastrophe is a critical antitumor strategy that can be achieved by various mechanisms that target the cell cycle (11). This work focused on a further exploration of the putative molecular activities of CCA-1.1 to inhibit cancer cells progression, also its effect on the mitochondrial respiration activity through two distinct models of breast cancer: triple-negative breast cancer (TNBC) MDA-MB-231 and human epidermal growth receptor-2 (HER2)-positive HCC1954 cells.

MATERIALS AND METHODS

Cell culture and compound

MDA-MB-231 and HCC1954 cells were obtained from American Type Culture Collection (ATCC®). The MDA-MB-231 cells were cultured in DMEM, while the latter cells were maintained in RPMI 1640 medium. Both were supplemented with 10% fetal calf serum (FCS) and 1% penicillin-streptomycin.

CCA-1.1 was obtained from the Cancer Chemoprevention Research Center, Faculty of Pharmacy, Universitas Gadjah Mada, Indonesia. The compounds were diluted in dimethyl sulfoxide (DMSO) as a stock solution and diluted in a medium before use. The maximum final concentration of DMSO in the medium was less than 0.5%.

Cytotoxicity and proliferative assay

To determine the half-growth inhibitory concentration (GI_{50}) among all cell lines, 2×10^4 cells/mL were seeded in a 35 mm dish, incubated for 24 h, then treated with a series of concentrations of CCA-1.1 (1 - 10 µM). After 4 days of incubation, the cells were harvested with trypsin-EDTA, and the viable cells and dead cells were counted using the trypan blue (Wako®, Japan) dye method.

To determine the irreversible effect of CCA-1.1 to inhibit cancer cells proliferation upon removal of the compound in the medium, cells were treated with 2 µM CCA-1.1 for 3 days, followed by a drug washout by replacing with a fresh medium (without CCA-1.1) for the next 2 days. The viable and dead cells from CCA-1.1 and untreated groups were stained with trypan blue and counted daily.

Flowcytometry-based assays

Cells (3×10^5 cells/mL) were treated with 2 µM CCA-1.1, and at the indicated time (24, 48, and 72 h), cells were harvested and washed with phosphate buffer saline (PBS). The cells were stained with propidium iodide (Sigma®, USA) solution (containing RNase A and Triton® X-100) for 30 min. The cell suspension was filtered in a cell strainer cap and collected in a tube, and the cells were monitored for cell cycle profile in FACSCalibur® flow cytometer and then analyzed to compare the distribution of cells against the untreated group using Cell Quest software.

For ROS level determination, 1×10^5 cells were pretreated with 20 µM 2,7-dichlorofluorescein diacetate (DCFDA; Sigma®, USA) for 30 min and treated with 2 µM CCA-1.1. Cells were filtered with a cell-strainer cap at indicated intervals before being subjected to a flow cytometer.

Mitotic index determination

After the treatment with 2 µM CCA-1.1, the cells were incubated with hypotonic shock (0.075 M KCl) for 6 min. After centrifugation, the cells were fixed in a mixture of acetic acid and methanol (1:3 v/v) and dropped on sterile microscope slides. The slides were airdried for 30-45 min before being stained by Hoechst 33324 and observed under a confocal microscope. In another experiment, the cells on the microscope slide were incubated with May-Grünwald solution (Merck®, Germany) for 5 min. The slides were washed with phosphate buffer for 1.5 min before being placed in Giemsa solution (Merck®, Germany) for

20 min. The slides were rinsed briefly in deionized water before being observed and captured under a phase-contrast microscope.

Senescence-associated β-galactosidase assay

The 2 µM CCA-1.1-treated cells were incubated with 4% formaldehyde solution for 10 min, rinsed with PBS 1 ×, stained using 0.2% X-gal (Wako®, Japan) solution, and incubated for 18 h before being observed under a phase-contrast microscope (12). The senescent and total cells in CCA-1.1 treatment and untreated groups were counted as calculated as the percentage of senescent cells.

Immunoblot

After the treatment with 2 µM CCA-1.1, the cells were collected to prepare whole-cell lysates using a lysis buffer containing phosphatase and protease inhibitors. The lysates were prepared in sample buffer before being loaded in 10% sodium dodecyl sulfate-polyacrylamide gel electrophoresis (SDS-PAGE), and the gel was then transferred onto polyvinylidene difluoride membranes (Immobilon, Merck®, Germany). The blots were blocked before being incubated at 4 °C overnight with primary antibodies purchased from Cell Signaling Technology® (USA), namely, phospho-cyclinB1 (Ser133; #4133), phospho-PLK1 (Thr210; #9062), phospho-aurora A kinase (Thr288; #3079), aurora A kinase (#12100), and β-actin antibody (#3700). These primary antibodies were diluted in 5% bovine serum albumin in tris buffer saline solution (with 0.05% of NaN_3; 1:500 v/v), except for β-actin which was diluted in 1:1000 v/v. After being washed with PBS-tween, the membrane was probed with an anti-mouse IgG secondary antibody (#NA931V) or protein-A HRP-linked antibody (#NA9120V) (Cytiva®, UK) for 1 h at room temperature. Detection was performed using enhanced chemiluminescence mixture (GE Life Science®, UK) and autoradiography film (Fujifilm®, Japan). The band was quantified in ImageJ and then compared against the untreated group.

Oxygen consumption rate profile

The cells were seeded in a dish for treatment with 2 µM CCA-1.1 for 24 h. A total of 2.25×10^5 cells for MDA-MB-231 cells and 1.5×10^5 cells for HCC1954 cells were collected in a 150 µL assay medium (DMEM medium added with 10 mM glucose, 1 mM pyruvate, and 2 mM glutamine) and distributed evenly in a miniplate that was already coated with Cell-Tak (Corning®). The microplate was spun down so the cells would attach to the coated well. Afterward, the microplate was incubated in a 37 °C incubator for 30 min. The sensor cartridge in the utility plate was added with Mito test kit reagents (Agilent®; 1.5 µM oligomycin, 1 µM FCCP, and 0.5 µM Rot/AA), and the oxygen consumption rate (OCR) profile was monitored for 75 min in XF HS mini analyzer (Agilent®, Germany). After analysis, the cells were lysed and quantified for total protein using the Bradford assay for normalizing OCR measurements. The normalization was then used for analyzing the maximal, basal, and ATP-linked respiration between untreated and CCA-1.1-treated cells.

Statistical analysis

Data were presented as mean ± standard deviation (SD) or standard error measurement (SEM), n = 3, and examined by statistical analysis between untreated and CCA-1.1 groups with unpaired t-test at a 95% confidence level in GraphPad Prism. *P*-values ≤ 0.05 were considered significant.

RESULTS

CCA-1.1 suppressed cells growth on MDA-MB-231 and HCC1954 cells

The current study aimed to evaluate the anticancer properties and molecular effect of CCA-1.1, particularly in MDA-MB-231 and HCC1954 breast cancer cells. First, CCA-1.1 demonstrated a suppressive effect on the cancer cells' growth and reflected by the GI_{50} score of 1.4 ± 1.08 µM and 1.2 ± 0.41 µM, respectively (Fig. 2A).

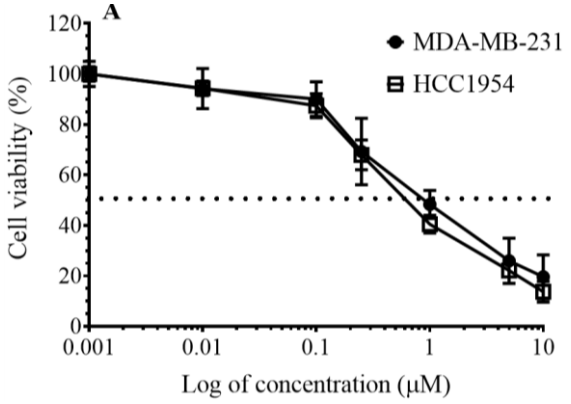

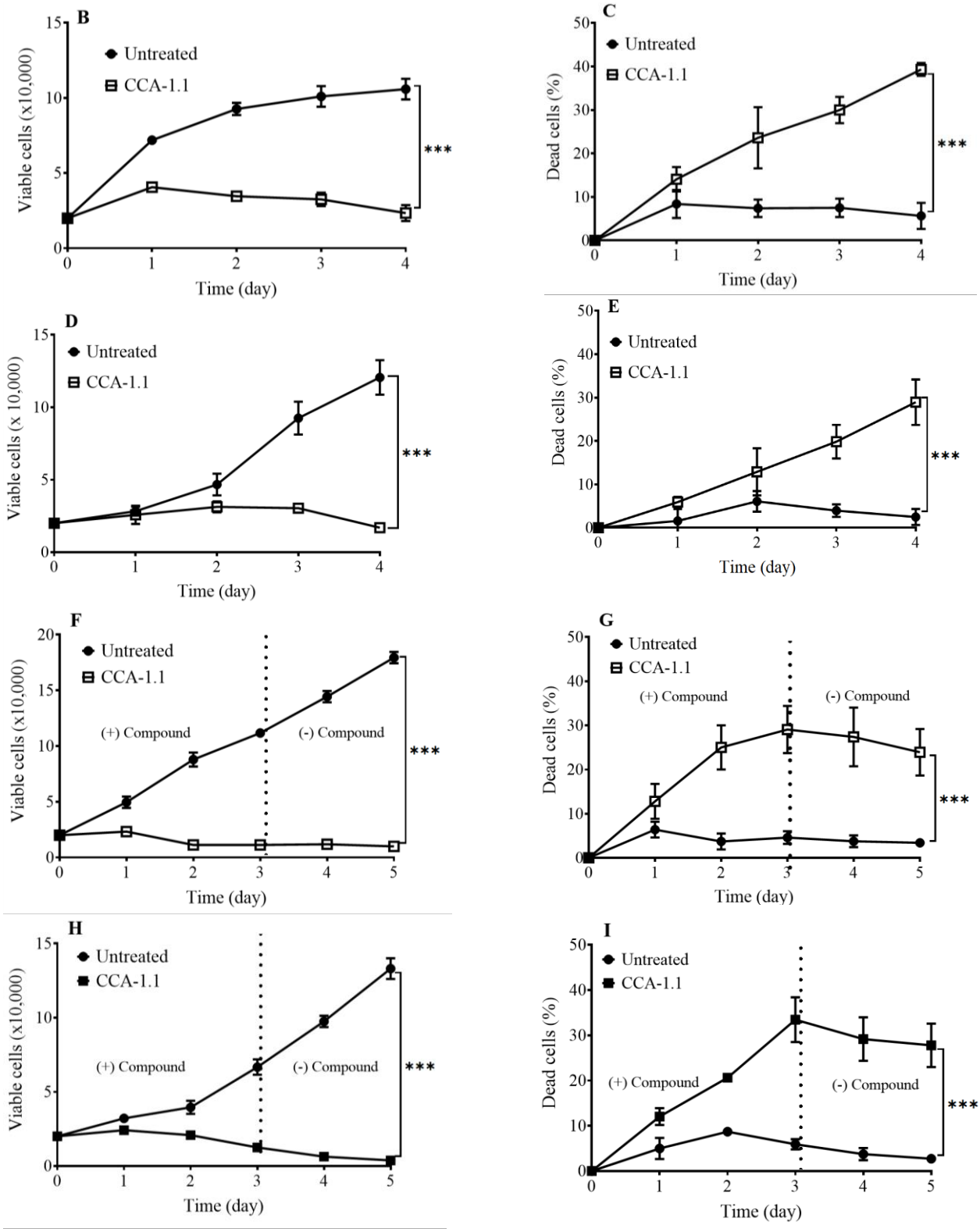

Fig. 2. CCA-1.1 suppressed the proliferation of breast cancer cells. (A) GI_{50} value of CCA-1.1 was assessed after 4-day treatment by cell counting with trypan blue exclusion assay from triplicate samples. Later, MDA-MB-231 cells were tested with 2 µM CCA-1.1 for 4 days, and the (B) viable and (C) dead cells were counted daily using the trypan blue exclusion method. HCC1954 cells were also incubated with 2 µM CCA-1.1 for 4 days, and the (D) viable and (E) dead cells were counted daily using the trypan blue exclusion method. In another experiment, MDA-MB-231 cells were treated with 2 µM CCA-1.1 for 3 days, and the medium containing drugs was then replaced with a fresh medium for the next 2 days. The (F) viable and (G) dead cells were counted daily and plotted into the graph. A similar experiment was also carried out for HCC1954 cells. The (H) viable and (I) dead cells were counted daily and plotted into the graph. The data were presented as mean ± SD, n = 3. ****P* < 0.001 Indicates significant differences compared to untreated cells. CCA-1.1, Chemoprevention curcumin analogue 1.1; GI_{50}, half growth inhibitory concentration

We then chose 2 µM for further assays. During the first 24 h, CCA-1.1 was quite inadequate to suppress the growth. However, after prolonged treatment, CCA-1.1 started to repress cell proliferation, followed by a higher percentage of dead cells (Fig. 2B-E). In a similar assay, CCA-1.1 was incubated for 3 days, then replaced with fresh medium to observe the antiproliferative effect upon the compound's removal. In both cells, the cytotoxic effect of CCA-1.1 was maintained as there was no indication of cell growth, while the dead cells remained stagnant (Fig. 2F-1I). These data implied that the suppressive activity with the irreversible effect of CCA-1.1 was also demonstrated in TNBC MDA-MB-231 and HER2-positive HCC1954 cells.

CCA-1.1 induced metaphase arrest in MDA-MB-231 and HCC1954 cells

Upon the antiproliferative effect presented by CCA-1.1, the cell cycle distribution was assessed in a time-course manner (24, 48, 72 h) toward MDA-MB-231 and HCC1954 cells through flow cytometry analysis. The G2/M population was increased under CCA-1.1 treatment for 24 h in MDA-MB-231 cells (ranging from 24.4% to 32.3%). CCA-1.1 might trigger mitotic failure as the polyploid cells were present in a more extended incubation period (9.9% at 48 h and 8.9% at 72 h). The subG1 population was detected after 72 h of treatment (9.4% *vs* 1.3% in the untreated group), which indicated CCA-1.1 induced DNA fragmentation ($N < 2$) (Fig. 3A and B). Quite different profile depicted in HCC1954-treated cells (Fig. 3C) as CCA-1.1 treatment significantly ($P < 0.05$) expanded the population of cells in the subG1 phase after 24 h (11.2% *vs* 4.7% in untreated), suggesting CCA-1.1 promoted cellular death in HCC1954 cells (Fig. 3D).

The follow-up assays were applied to determine the specific phase that CCA-1.1 inhibited in MDA-MB-231 and HCC1954 cells. Staining with May-Grünwald-Giemsa allowed the azure B (from Giemsa)-DNA complex to interact with eosin Y to produce purple colour (13). Some of the cells in the CCA-1.1-treated group display an intense purple colour because the nuclear membrane was dissembled, implying that CCA-1.1 might induce mitotic arrest (Fig. 3E). The quantitative analysis further showed that CCA-1.1 significantly induced cells into the mitotic phase (Fig. 3F and G). Hoechst staining was adopted to confirm the mitosis phase inhibited by CCA-1.1. As indicated by chromosome staining, we found that CCA-1.1 induced metaphase arrest in MDA-MB-231 and HCC1954 cells aligned in the equatorial plane (Fig. 3H). The mitotic index from the CCA-1.1 group was significantly higher than the untreated MDA-MB-231 cells (Fig. 2I). A similar result also occurred after treatment in HCC1954 cells that CCA-1.1 also induced mitotic arrest in metaphase (Fig. 3J). These findings implied that CCA-1.1 targeted metaphase to induce mitotic arrest in MDA-MB-231 and HCC1954 cells.

CCA-1.1 mediated mitotic arrest by modulating major mitotic kinases in aggressive breast cancer cells

Since we demonstrated that CCA-1.1 induced mitotic arrest, some mitotic regulator proteins were checked to determine whether the antiproliferative activity of CCA-1.1 affects their expression. Among those proteins, we chose aurora A, phosphorylated-aurora A kinase (p-aurora A), phosphorylated-polo kinase 1 (p-PLK1), and phosphorylated-cyclin B1 (p-CycB1) were evaluated after 24 h incubation with CCA-1.1 (Fig. 4A). The total protein level of aurora A kinase was suppressed in MDA-MB-231 but not in HCC1954 cells (Fig. 4B). However, the protein level of p-aurora A was not affected (even tended to increase) in both cell lines (Fig. 4C). The phosphorylation of PLK1 tended to elevate in CCA-1.1 treatment for 24 h in MDA-MB-231 and HCC1954 cells (Fig. 4D), indicating that the action of CCA-1.1 peaked during mitosis. The cyclin B1 phosphorylation was also observed in both treated cells (Fig. 4E). These data implied that CCA-1.1 activity in mitosis correlated with the level of mitotic regulatory proteins toward MDA-MB-231 and HCC1954 cells.

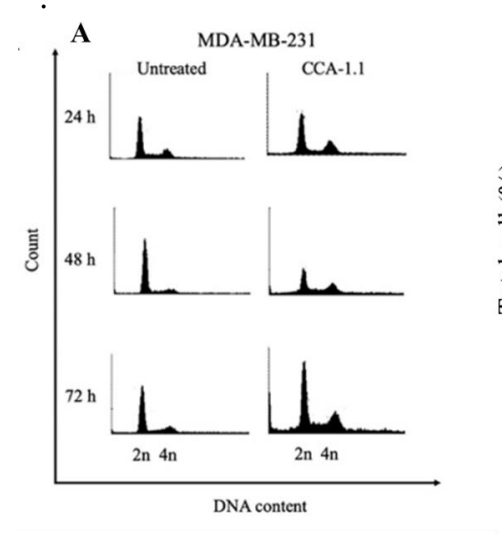
A
MDA-MB-231
Untreated
CCA-1.1
24 h
48 h
72 h
Count
2n 4n
2n 4n
DNA content

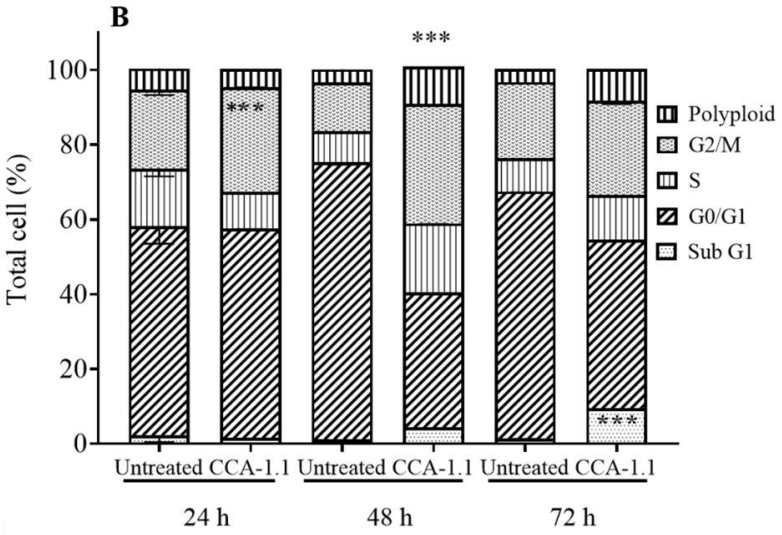
B
***
Total cell (%)
Polyploid
G2/M
S
G0/G1
Sub G1
Untreated CCA-1.1 Untreated CCA-1.1 Untreated CCA-1.1
24 h
48 h
72 h

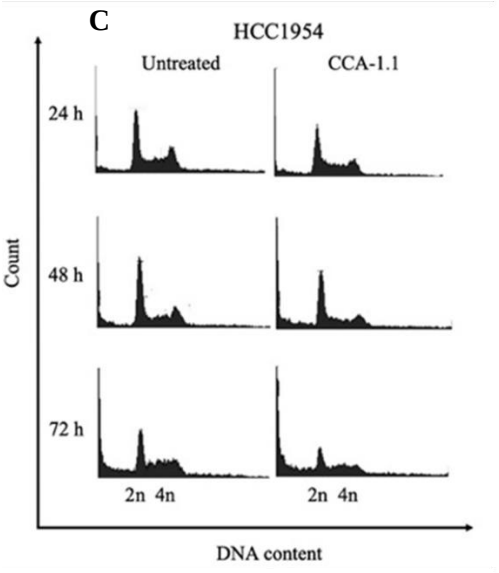
C
HCC1954
Untreated
CCA-1.1
24 h
48 h
72 h
Count
2n 4n
2n 4n
DNA content

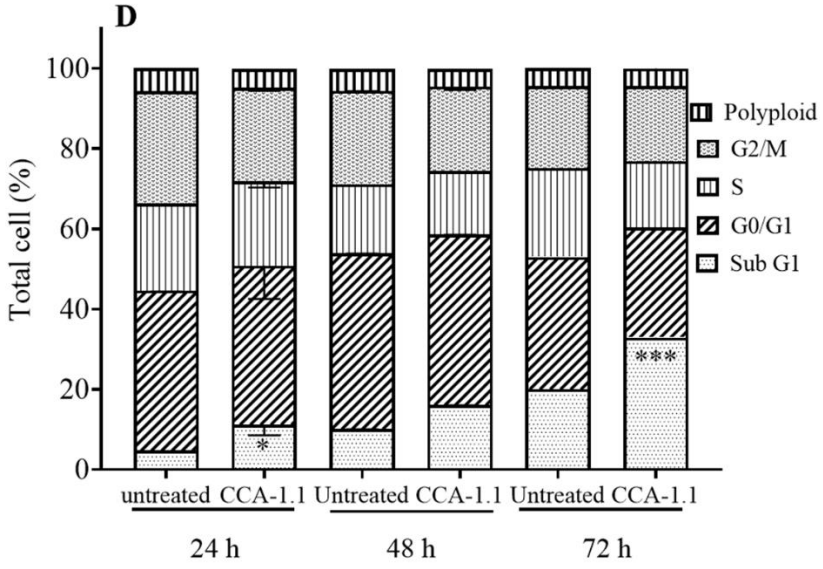
D
Total cell (%)
Polyploid
G2/M
S
G0/G1
Sub G1
untreated CCA-1.1 Untreated CCA-1.1 Untreated CCA-1.1
24 h
48 h
72 h

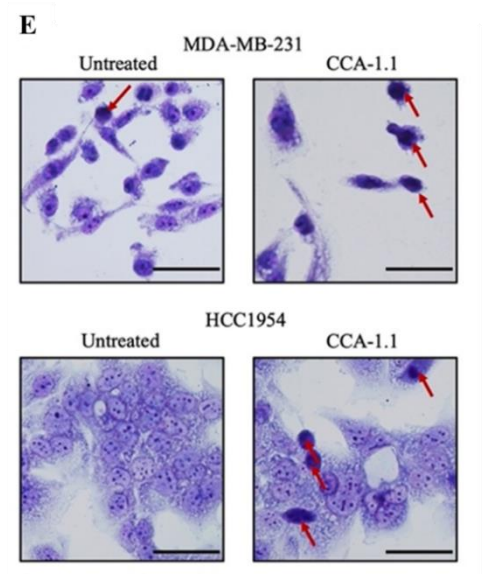
E
MDA-MB-231
Untreated
CCA-1.1
HCC1954
Untreated
CCA-1.1

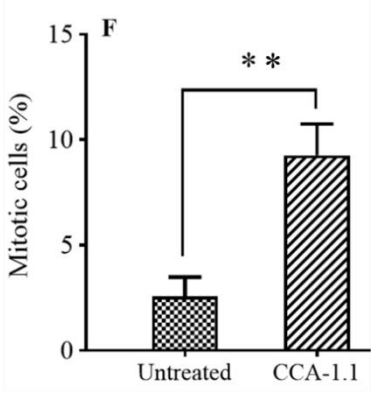
F
**
Mitotic cells (%)
Untreated
CCA-1.1

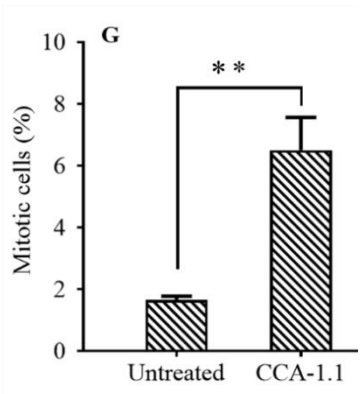
G
**
Mitotic cells (%)
Untreated
CCA-1.1

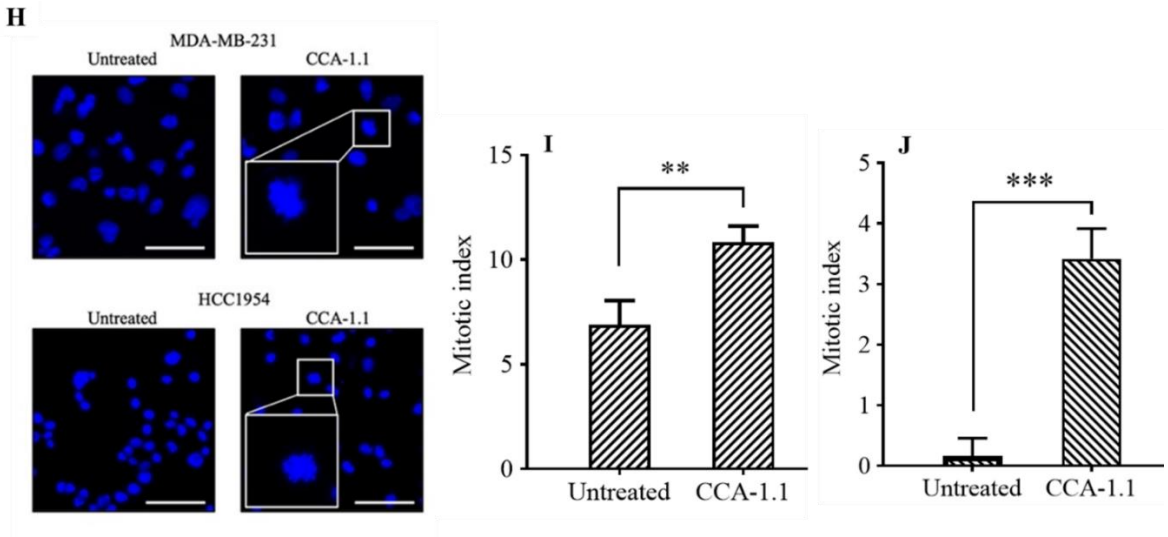

Fig. 3. CCA-1.1 induced cell arrest at the G2/M phase on MDA-MB-231 and HCC1954 cells. Each MDA-MB-231 and HCC1954 cell line (3×10^5 cells/mL) was seeded in a 35 mm dish and treated with 2 µM CCA-1.1 for 24, 48, and 72 h. Upon the interval of incubation, the cells were stained with propidium iodide solution and analyzed for the cell profile using a flow cytometer. (A) Cell cycle profile in MDA-MB-231 cells treated with CCA-1.1 and (B) quantification of cell population in each cell cycle phase. (C) Cell cycle profile in HCC1954 cells treated with CCA-1.1 and (D) quantification of HCC1954 cell population in every cell cycle phase. (E) May-Grünwald-Giemsa stain for the cells treated with 2 µM CCA-1.1 after 24 h on MDA-MB-231 and HCC1954 cells. The morphology of cells after staining was observed under a phase-contrast microscope (scale bar 20 µm). (F) The percentage of mitotic cells in MDA-MB-231 cells was determined by dividing the number of mitotic cells against the total cell number. (G) Percentage of mitotic cells in HCC1954-treated cells. The red arrow marked the presence of the mitotic cells. (H) Mitotic spread from MDA-MB-231 and HCC1954 cells treated with CCA-1.1 24 h. The cells were fixed, stained with Hoechst 33342, and observed under a confocal microscope, scale bar 50 µm. (I) The mitotic index was quantified by dividing the mitotic cell against the total number of MDA-MB-231 cells. (J) The mitotic index after treatment in HCC1954 cells. The white grid box presented the metaphase-arrest cell. The data were displayed as mean ± SD, n= 3. **P* < 0.05, ***P* < 0.01, ****P* < 0.001 Indicate significant differences compared to untreated cells. CCA-1.1, Chemoprevention curcumin analog 1.1.

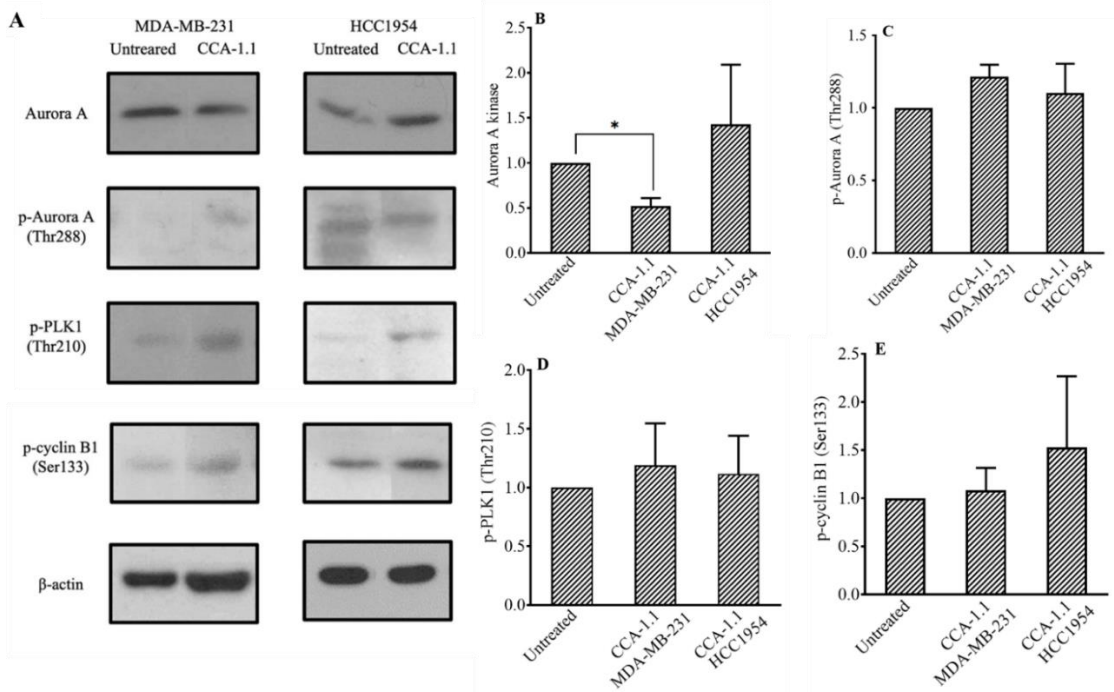

Fig. 4. Mitotic regulatory protein kinase phosphorylation is affected by treatment with CCA-1.1 in MDA-MB-231 and HCC1954 cells. (A) Immunoblot analysis of MDA-MB-231 or HCC1954 cell lysates after treatment with 2 µM CCA-1.1 for 24 h. Western blot was employed using the antibodies against pThr210-PLK1, pSer133-cyclinB1, pThr288-aurora A, and aurora A kinase. β-actin served as a loading control for western blot. Band intensity was semi-quantified using ImageJ for (B) aurora A kinase, (C) p-Aurora A, (D) p-PLK1, and (E) p-cyclin B1. The data were presented as mean ± SD, n = 3. **P* < 0.05 Indicates significant differences compared to untreated cells. CCA-1.1, Chemoprevention curcumin analog 1.1.

CCA-1.1 induced senescence in MDA-MB-231 and HCC1954 cells

Given that the cells treated with CCA-1.1 were irreversibly arrested at the mitosis, this phenomenon's possible mechanism warrants further exploration. The mitotic arrest could also be followed by mitotic slippage prior to senescence (11). Therefore, CCA-1.1 was also evaluated for a similar effect on cellular senescence. The senescence phenotype can be visualized as the green-stained cells resulting from the lysosomal β-galactosidase activity. The 24-h treatment of CCA-1.1 in MDA-MB-231 cells significantly increased the number of senescent cells by 17.9% (Fig. 5A and B). This phenomenon was also observed in HCC1954 cells (Fig. 5C), as the untreated group generated 10.0% of senescent cells, and this number significantly increased to 27.9% after incubation with CCA-1.1 (Fig. 5D). These results convinced that cell viability suppression and prolonged cell cycle arrest could also be correlated with senescence induction in response to CCA-1.1 treatment.

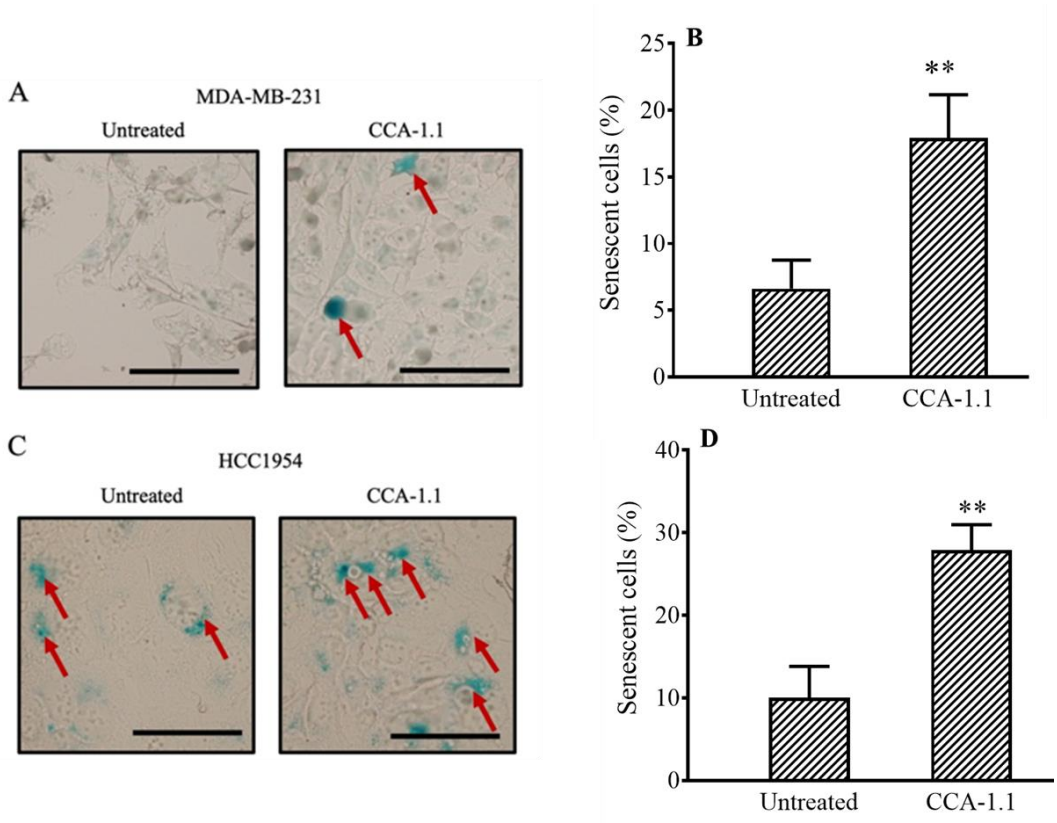

Fig. 5. CCA-1.1 treatment for 24 h induced cellular senescence in MDA-MB-231 and HCC1954 cells. 2 × 10^5 MDA-MB-231 and HCC1954 cells were cultured in a 35 mm petri dish and later treated with 2 µM CCA-1.1 for 24 h. Cells were fixed and incubated with SA-β-Gal, and the senescence activity was observed under a phase-contrast microscope, scale bar 20 µm. (A) After treatment in MDA-MB-231 cells, the red arrow marks the green-stained cells indicating the presence of senescent cells. (B) Percentage of senescent cells in CCA-1.1-treated MDA-MB-231 cells. (C) Senescence evidence after treatment with CCA-1.1 in HCC1954 cells, with the red arrow marking the appearance of senescent cells. (D) Percentage of senescent cells in treated HCC1954 cells. The data were presented as mean ± SD, n = 3. $^{**}P < 0.01$ Indicates significant differences compared to untreated cells. CCA-1.1, Chemoprevention curcumin analogue 1.1.

CCA-1.1 modulated ROS generation and disrupted mitochondria respiration

Several studies reported that the role of ROS in senescence had been attributed to cancer (14-16). This work measured ROS level in five interval hours (2, 4, 8, 18, and 24 h). CCA-1.1 maintained higher ROS levels during 4, 8, and 24 h incubation, while lower at 2 and 18 h after treatment in MDA-MB-231 cells (Fig. 6A). A distinct phenomenon was presented in HCC1954 cells, in which the ROS level of CCA-1.1-treated cells was significantly elevated since earlier hours and maintained a high level even after 24 h (Fig. 6B). These results suggested that ROS could also contribute to the mitosis arrest and senescence induction by CCA-1.1

Elevated ROS levels at some point also mediated dysfunction in the mitochondria (17) and caused damage to the mitochondrial respiratory chain (18). To evaluate the effect of CCA-1.1 on mitochondria function, cellular OCR was monitored as an indicator of mitochondrial respiration (Fig. 6C and D), along with three associated parameters (basal respiration, maximal respiration, and ATP-linked respiration). CCA-1.1 increased the maximal respiration and suppressed the basal respiration but did not affect ATP-linked respiration in MDA-MB-231 cells (Fig. 6E-G). CCA-1.1 was also tested for its effect on mitochondria respiration in HCC1954 cells after 24 h of incubation. The results showed that all the parameters were not altered (Fig. 6H-J) in the treatment groups compared with those in the untreated group. All these data demonstrate that CCA-1.1 was mainly induced ROS production, which later causes mitochondrial impairment.

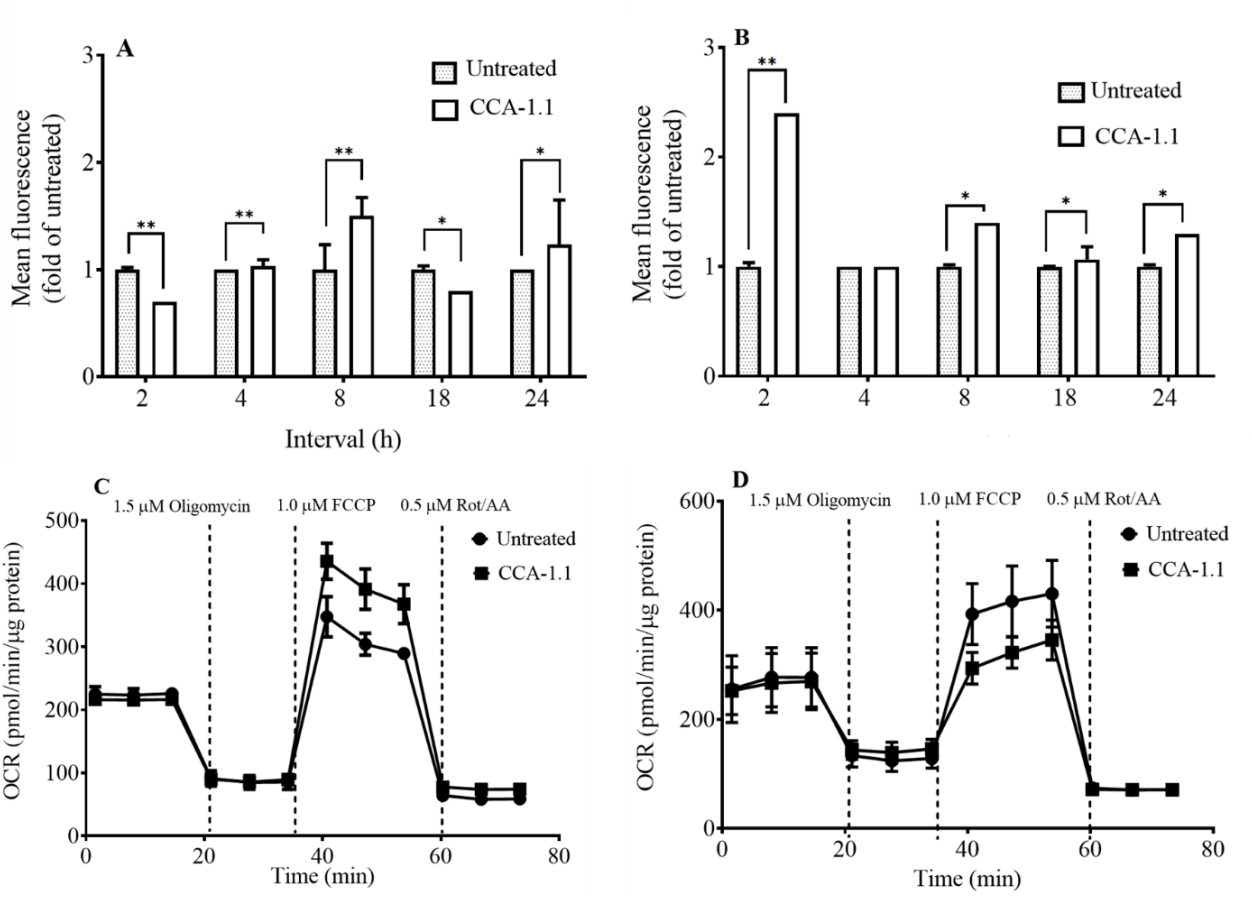

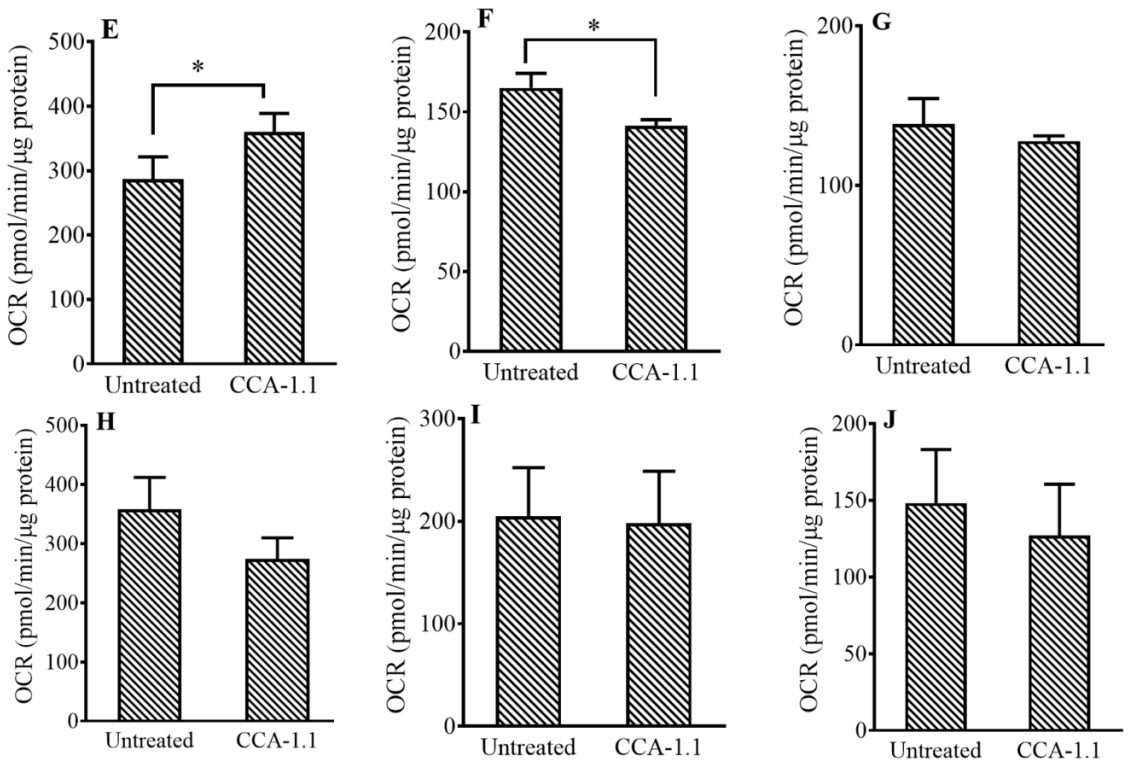

Fig. 6. CCA-1.1 treatment increased the accumulation of intracellular ROS levels and its effect on mitochondrial respiration of MDA-MB-231 and HCC1954 cells. A total of 1×10^5 cells/mL were grown for 24 h and then harvested. Cells were stained with 20 µM DCFDA 30 min prior to incubation with 2 µM CCA-1.1. Total ROS levels after 2, 4, 8, 18, and 24 h in (A) MDA-MB-231 and (B) HCC1954 cells were measured using a flow cytometer. The metabolic profile of (C) MDA-MB-231 cells and (D) HCC1954 cells upon treatment with 2 µM CCA-1.1 for 24 h were assessed using the Seahorse XF HS mini analyzer. The OCR level graph displayed from the experiments in MDA-MB-231 treated with CCA-1.1, along with the parameters of (E) maximal respiration, (F) basal respiration, and (G) ATP-linked respiration. Mitochondria respiration after treatment with CCA-1.1 for 24 h was also determined in HCC1954 cells using the parameters of (H) maximal respiration, (I) basal respiration, and (J) ATP-linked respiration. The data were presented as mean ± SD, n = 3. **P* < 0.05 and ***P* < 0.01 Indicate significant differences compared to untreated cells. CCA-1.1, Chemoprevention curcumin analog 1.1; ROS, reactive oxygen species; OCR, oxygen consumption rate

DISCUSSION

The current work presented the anticancer activities of CCA-1.1 using MDA-MB-231 (TNBC) and HCC1954 (HER2-positive) breast cancer cells. The cytotoxic effect from CCA-1.1 had been reported in other studies that also used breast cancer cells, including luminal MCF7 (19) and T47D cells (4), TNBC 4T1 and MCF7/HER2 cells (2,20). CCA-1.1 inhibited cell growth irreversibly and receded the possibility of cancer recurrence upon withdrawal of CCA-1.1 in both MDA-MB-231 and HCC1954 cells. The activity of CCA-1.1 in the cell cycle has been documented in prior studies (2,4), but this is the first study investigating the specific phase inhibited by CCA-1.1. Unlike MDA-MB-231 cells, the polyploid cells did not present in the cell cycle profile after treatment in the HCC1954 cell because some of the treated cells had already accumulated in the subG1 phase, indicating that these compounds were more sensitive in HCC1954 than MDA-MB-231 at the same tested concentration. SubG1 populations are commonly linked to apoptosis incidence because of the reduced DNA content as the essential characteristic of apoptotic cells (21).

The percentage of hyperploid MDA-MB-231 cells increased during the more prolonged incubation with the compound. This finding suggested that CCA-1.1 might induce mitotic catastrophe when cells cannot complete the mitosis cycle because of defects during mitosis entry (22). We found that CCA-1.1 perturbed G2/M arrest and further assessment confirmed that this compound halted during metaphase. The prolonged arrest in metaphase might trigger spindle assembly checkpoint activation, causing cyclin B1 phosphorylation to stabilize (23).

This phenomenon might explain why the phosphorylation of cyclin B1 remained active in CCA-1.1 treated cells even though they induce metaphase arrest. Moreover, one of the prominent biochemical features of mitotic catastrophe is an abnormal increase of cyclin B1 (24).

The phosphorylation of PLK1 was seen in CCA-1.1-treated cells, which confirmed that CCA-1.1 activities peaked in mitosis. In metaphase, PLK1 helps maintain kinetochore-microtubule attachment stability (25). Since this study investigated the physiology molecular of CCA-1.1 in mitosis, the well-known regulator aurora A kinase was also evaluated at the protein level. CCA-1.1 inhibited the protein level of aurora A in MDA-MB-231 cells, yet the phosphorylation of aurora A in Thr288 presented an unchanged level compared with the untreated group. Even with the low protein level, the phosphorylation of aurora A still allowed for the recruitment of γ-tubulin, though the centriole separation began to disrupt, resulting in the dysfunction of the centrosome (26). Furthermore, aurora A kinase also acts as the primary activator for PLK1 in mitosis, the activity of PLK1 is also maintained if there is aurora A activity (27).

In the case of CCA-1.1, the cells passed the prometaphase to metaphase, but likely with the improper chromosome aligned in the equatorial plate because the inhibition of aurora A interferes with the ability of the chromosome to align and causes metaphase arrest in breast cancer cells. A recent molecular docking analysis study illustrated that CCA-1.1 bound with the ATP pocket site in the adenine-binding region (Leu139), and the hydroxyl in its benzene ring engaged with residue Ala213 located in the hinge region that is responsible for catalytic active site formation of aurora A (5,28). These phenomena are quite different from the mechanism presented by Alisertib (MLN8237), a selective aurora A inhibitor currently undergoing clinical trial studies (29,30). The study by Li *et al.* (31) demonstrated that MLN8237 induced G2/M arrest through suppression of CDK1 and cyclin B1, followed by upregulation of p21 and p53, which attributed to induce cellular death *via* apoptosis in MDA-MB-231 cells. Hence, CCA-1.1 deserves the chance for further development as a potential antimitotic drug.

At some point, the mitotic catastrophe is also associated with cell aging or senescence (32). The morphological-marker mitotic catastrophic process also promotes or occurs parallel to cellular senescence. In some instances, the defects cause mitotic exit and induce cell senescence through mitotic catastrophe (33,34) because, in p53-mutated cells, some cell cycle checkpoints become compromised (10). It is known that many chemotherapies produce ROS and are partly responsible for inducing senescence (14). CCA-1.1 mainly escalated the intracellular ROS level throughout 24 h, which might have led to the increased number of senescent cells.

The ROS also amplifies the stress signaling that imbalance the redox system with the primary target in mitochondria to provide tumor proliferation. However, when the ROS level outpaces the reduction capacity in cancer cells, the nucleus and mitochondria will be damaged (35). Notably, CCA-1.1 suppressed the basal respiratory in MDA-MB-231 cells, indicating the potential for mitochondrial dysfunction. The acute oxidative stress is because the drug treatment might enhance ROS levels, induce mitochondrial dysfunction in TNBC cells, some mediators to release from mitochondria and initiate programmed cell death (apoptosis) (36). These findings could be worth studying in the future to better understand the mechanism of CCA-1.1 in mitochondria. Reckoning with the prior reports that revealed that CCA-1.1 exhibited more cytotoxic effect than curcumin (37), followed by the synergistic effect of CCA-1.1 with doxorubicin in T47D, 4T1, and MCF7/HER2 cancer cells (4,20) or in combination with PGV-1 in CML K562 cells (5), there is an opportunity to also combining this curcumin analog with another existing chemotherapy with different molecular targets to enhance the efficacy of eliminating aggressive breast cancer cells.

CONCLUSION

Given these results, this study proposed the putative molecular mechanism of CCA-1.1 in MDA-MB-231 and HCC1954 cells: induce metaphase arrest, enhance intracellular ROS level in cancer cells, mediate senescence and mitochondria dysfunction. Further exploration

is essential to investigate the molecular-based mechanism underlying the anti-tumorigenic effect of CCA-1.1, focusing on centrosome proteins that may interfere with mitotic arrest or the effect on ROS-metabolizing enzymes.

Acknowledgments

We are grateful to the IIDA scholarship for supporting the student research exchange program at NAIST. This study is partially supported by Master Education Leading to Doctoral Program for Excellent Graduate (PMDSU) Research Scheme from the Ministry of Education, Culture, Research, and Technology, Republic of Indonesia (granted to Dr. Edy Meiyanto).

Conflict of interest statements

All authors declared no conflict of interest in this study

Authors' contribution

E. Meiyanto conceived the original idea, supervised, and funded the project; J. Kato and R.I. Jenie supervised the project; D. Novitasari performed all the experiments. The final version of the article was approved by all authors.

REFERENCES

1. Utomo RY, Wulandari F, Novitasari D, Lestari B, Susidarti RA, Jenie RI, *et al*. Preparation and cytotoxic evaluation of PGV-1 derivative, CCA-1.1, as a new curcumin analog with improved-physicochemical and pharmacological properties. Adv Pharm Bull. 2022;12(3):603-612. DOI: 10.34172/apb.2022.063.
2. Novitasari D, Jenie RI, Wulandari F, Putri DDP, Kato J, Meiyanto E. a curcumin like structure (CCA-1.1) induces permanent mitotic arrest (senescence) on triple negative breast cancer (TNBC) cells, 4T1. Res J Pharm Technol. 2021;14(8):4375-482. DOI: 10.52711/0974-360X.2021.00760
3. Wulandari F, Ikawati M, Kirihata M, Kato JY, Meiyanto E. A new curcumin analog, CCA-1.1, induces cell death and cell cycle arrest in WiDr colon cancer cells via ROS generation. J Appl Pharm Sci. 2021;11(10):99-105. DOI: 10.7324/JAPS.2021.1101014
4. Wulandari F, Ikawati M, Novitasari D, Kirihata M, Kato J, Meiyanto E. New curcumin analog, CCA-1.1, synergistically improves the antiproliferative effect of doxorubicin against T47D breast cancer cells. Indonesian J Pharm. 2020;31(4):244-256. DOI: https://doi.org/10.22146/ijp.681.
5. Meiyanto E, Novitasari D, Utomo RY, Susidarti RA, Putri DDP, Kato J. Bioinformatic and molecular interaction studies uncover that CCA-1.1 and PGV-1 differentially target mitotic regulatory protein and have a synergistic effect against leukemia cells. Indones J Pharm. 2022;33(2):225-233. DOI: 10.22146/ijp.3382.
6. Novitasari D, Jenie RI, Kato J, Meiyanto E. The integrative bioinformatic analysis deciphers the predicted molecular target gene and pathway from curcumin derivative CCA-1.1 against triple-negative breast cancer (TNBC). J Egypt Natl Cancer Inst. 2021;33(1):19,1-10. DOI: 10.1186/s43046-021-00077-1.
7. Novitasari D, Jenie RI, Kato J, Meiyanto E. Network pharmacological analysis identifies the curcumin analog CCA-1.1 targeting mitosis regulatory process in HER2-positive breast cancer. Indonesian J Pharm. 2023;34(1):54-64. DOI: 10.22146/ijp.4453
8. Khongkow P, Gomes AR, Gong C, Man EPS, Tsang JWH, Zhao F, *et al*. Paclitaxel targets FOXM1 to regulate KIF20A in mitotic catastrophe and breast cancer paclitaxel resistance. Oncogene. 2016;35(8):990-1002. DOI: 10.1038/onc.2015.152.
9. Morse DL, Gray H, Payne CM, Gillies RJ. Docetaxel induces cell death through mitotic catastrophe in human breast cancer cells. Mol Cancer Ther. 2005;4(10):1495-1504. DOI: 10.1158/1535-7163.MCT-05-0130.
10. Ianzini F, Mackey MA. Mitotic catastrophe. In: Gewirtz DA, Holt SE, Grant S, editors. Apoptosis, senescence, and cancer. Totowa, NJ: Humana Press; 2007. P. 73-91 DOI: 10.1007/978-1-59745-221-2_4
11. Mc Gee MM. Targeting the mitotic catastrophe signaling pathway in cancer. Mediators Inflamm. 2015;2015:146282,1-13. DOI: 10.1155/2015/146282.
12. Larasati YA, Yoneda-Kato N, Nakamae I, Yokoyama T, Meiyanto E, Kato J. Curcumin targets multiple enzymes involved in the ROS metabolic pathway to suppress tumor cell growth. Sci Rep. 2018;8(1):2039,1-13. DOI: 10.1038/s41598-018-20179-6
13. Horobin R. How Romanowsky stains work and why they remain valuable - including a proposed universal Romanowsky staining mechanism and a rational troubleshooting scheme. Biotech Histochem. 2011;86(1):36-51. DOI: 10.3109/10520295.2010.515491
14. Davalli P, Mitic T, Caporali A, Lauriola A, D'Arca D. ROS, cell senescence, and novel molecular mechanisms in aging and age-related diseases. Oxid Med Cell Longev. 2016;2016:3565127,1-18. DOI: 10.1155/2016/3565127.
15. Lawless C, Jurk D, Gillespie CS, Shanley D, Saretzki G, Zglinicki T von, *et al*. A stochastic step model of replicative senescence explains ROS production rate

in aging cell populations. PLoS One. 2012;7(2):e32117,1-7.
DOI: 10.1371/journal.pone.0032117.
16. Passos JF, Nelson G, Wang C, Richter T, Simillion C, Proctor CJ, *et al*. Feedback between p21 and reactive oxygen production is necessary for cell senescence. Mol Syst Biol. 2010;6:347,1-14.
DOI: 10.1038/msb.2010.5.
17. Perillo B, Di Donato M, Pezone A, Di Zazzo E, Giovannelli P, Galasso G, *et al*. ROS in cancer therapy: the bright side of the moon. Exp Mol Med. 2020;52(2):192-203.
DOI: 10.1038/s12276-020-0384-2
18. Sullivan LB, Chandel NS. Mitochondrial reactive oxygen species and cancer. Cancer Metab. 2014;2:17,1-12.
DOI: 10.1186/2049-3002-2-17.
19. Novitasari D, Wulandari F, Jenie RI, Utomo RY, Kato JY, Meiyanto E. A new curcumin analog, CCA-1.1, induces cell cycle arrest and senescence toward ER-positive breast cancer cells. Int J Pharm Res. 2021;13(1):1-9.
DOI: 10.31838/ijpr/2021.13.01.002.
20. Novitasari D, Jenie RI, Utomo RY, Kato JY, Meiyanto E. CCA-1.1, a novel curcumin analog, exerts cytotoxic anti- migratory activity toward TNBC and HER2-enriched breast cancer cells. Asian Pac J Cancer Prev. 2021;22(6):1827-1836.
DOI: 10.31557/APJCP.2021.22.6.1827.
21. Plesca D, Mazumder S, Almasan A. DNA damage response and apoptosis. Methods Enzymol. 2008;446:107-122.
DOI: 10.1016/S0076-6879(08)01606-6.
22. Sazonova EV, Petrichuk SV, Kopeina GS, Zhivotovsky B. A link between mitotic defects and mitotic catastrophe: detection and cell fate. Biol Direct. 2021;16(1):25,1-11.
DOI: 10.1186/s13062-021-00313-7
23. Musacchio A. The molecular biology of spindle assembly checkpoint signaling dynamics. Curr Biol. 2015;25(20):R1002-1018.
DOI: 10.1016/j.cub.2015.08.051
24. Harley ME, Allan LA, Sanderson HS, Clarke PR. Phosphorylation of Mcl-1 by CDK1-cyclin B1 initiates its Cdc20-dependent destruction during mitotic arrest. EMBO J. 2010;29(14):2407-2420.
DOI: 10.1038/emboj.2010.112.
25. Schmucker S, Sumara I. Molecular dynamics of PLK1 during mitosis. Mol Cell Oncol. 2014;1(2):e954507,1-9.
DOI: 10.1080/23723548.2014.954507 PMID: 27308323
26. Marumoto T, Honda S, Hara T, Nitta M, Hirota T, Kohmura E, *et al*. Aurora-A kinase maintains the fidelity of early and late mitotic events in HeLa cells. J Biol Chem. 2003;278(51):51786-5195.
DOI: 10.1074/jbc.M306275200
27. Asteriti IA, De Mattia F, Guarguaglini G. Cross-talk between AURKA and Plk1 in mitotic entry and spindle assembly. Front Oncol. 2015;5:283,1-9.
DOI: 10.3389/fonc.2015.00283
28. Cheetham GMT, Knegtel RMA, Coll JT, Renwick SB, Swenson L, Weber P, *et al*. Crystal structure of aurora-2, an oncogenic serine/threonine kinase. J Biol Chem. 2002;277(45):42419-4222.
DOI: 10.1074/jbc.C200426200.
29. Manfredi MG, Ecsedy JA, Chakravarty A, Silverman L, Zhang M, Hoar KM, *et al*. Characterization of Alisertib (MLN8237), an investigational small-molecule inhibitor of aurora A kinase using novel *in vivo* pharmacodynamic assays. Clin Cancer Res. 2011;17(24):7614-7624.
DOI: 10.1158/1078-0432.CCR-11-1536
30. Melichar B, Adenis A, Lockhart AC, Bennouna J, Dees EC, Kayaleh O, *et al*. Safety and activity of alisertib, an investigational aurora kinase A inhibitor, in patients with breast cancer, small-cell lung cancer, non-small-cell lung cancer, head and neck squamous-cell carcinoma, and gastro-oesophageal adenocarcinoma: a five-arm phase 2 study. Lancet Oncol. 2015;16(4):395-405.
DOI: 10.1016/S1470-2045(15)70051-3.
31. Li JP, Yang YX, Liu QL, Pan ST, He ZX, Zhang X, *et al*. The investigational aurora kinase A inhibitor alisertib (MLN8237) induces cell cycle G2/M arrest, apoptosis, and autophagy *via* p38 MAPK and Akt/mTOR signaling pathways in human breast cancer cells. Drug Des Devel Ther. 2015;9:1627-1652.
DOI: 10.2147/DDDT.S75378.
32. Bianchi-Smiraglia A, Nikiforov MA. Controversial aspects of oncogene-induced senescence. Cell Cycle. 2012;11(22):4147-4151.
DOI: 10.4161/cc.22589.
33. Li H, Hu P, Wang Z, Wang H, Yu X, Wang X, *et al*. Mitotic catastrophe and p53-dependent senescence induction in T-cell malignancies exposed to nonlethal dosage of GL-V9. Arch Toxicol. 2020;94(1):305-323.
DOI: 10.1007/s00204-019-02623-2
34. Vitale I, Galluzzi L, Castedo M, Kroemer G. Mitotic catastrophe: a mechanism for avoiding genomic instability. Nat Rev Mol Cell Biol. 2011;12(6):385-392.
DOI: 10.1038/nrm3115.
35. Kuczler MD, Olseen AM, Pienta KJ, Amend SR. ROS-induced cell cycle arrest as a mechanism of resistance in polyaneuploid cancer cells (PACCs). Prog Biophys Mol Biol. 2021;165:3-7.
DOI: 10.1016/j.pbiomolbio.2021.05.002.
36. Pelicano H, Zhang W, Liu J, Hammoudi N, Dai J, Xu RH, *et al*. Mitochondrial dysfunction in some triple-negative breast cancer cell lines: role of mTOR pathway and therapeutic potential. Breast Cancer Res. 2014;16(5):434,1-16.
DOI: 10.1186/s13058-014-0434-6.
37. Moordiani M, Novitasari D, Susidarti RA, Kato J, Meiyanto E. Curcumin analogs PGV-1 and CCA-1.1 induce cell cycle arrest in human hepatocellular carcinoma cells with overexpressed MYCN. Indones Biomed J. 2023;15(2):141-149.
DOI: 10.18585/inabj.v15i2.2147.